# REPORT DOCUMENTATION PAGE

Form Approved
OMB No. 0704-0188



| 1. AGENCY USE ONLY (Leave blank) | 2. REPORT DATE | 3. REPORT TYPE AND DATES COVERED |
|---|---|---|
| | January 12, 1996 | Tech Rpt. # 25 |

**4. TITLE AND SUBTITLE**
Magnetic Behavior of New Ce-Pd-Sn Ternary Compounds

**5. FUNDING NUMBERS**
N00014-93-1-0904
Dr. John Pazik
R&T: 3134037ess08

**6. AUTHOR(S)**
R.A. Gordon and F.J. DiSalvo

**7. PERFORMING ORGANIZATION NAME(S) AND ADDRESS(ES)**
Department of Chemistry
Cornell University
Ithaca, NY 14853-1301

**8. PERFORMING ORGANIZATION REPORT NUMBER**

**9. SPONSORING/MONITORING AGENCY NAME(S) AND ADDRESS(ES)**
Office of Naval Research
Chemistry Program
800 N. Quincy St.
Alexandria, VA 22217

**10. SPONSORING/MONITORING AGENCY REPORT NUMBER**

**11. SUPPLEMENTARY NOTES**



**12a. DISTRIBUTION/AVAILABILITY STATEMENT**
This document has been approved for public release and sale; its distribution is unlimited

**12b. DISTRIBUTION CODE**

**13. ABSTRACT** (Maximum 200 words)

We have prepared and measured the magnetic susceptibility of several new ternary compounds in the Ce-Pd-Sn system: $CePd_{0.5}Sn_2$, $Ce_8Pd_{24}Sn$, "$Ce_4Pd_7Sn_4$" and the solid solution based on $Ce_2Pd_2Sn$. In $CePd_{0.5}Sn_2$, an effective magnetic moment of 2.60(3)μB is observed but no ordering is apparent above 4.2K. Complete nickel substitution for Pd in $Ce(Pd_{1-x}Ni_x)_{0.5}Sn_2$ results in the known lower limit to the $CeNi_{1-x}Sn_2$ solid solution. We have determined the extent of the solid solution based on $Ce_2Pd_2Sn$ to have the form $Ce_4Pd_{4+2x}Sn_{2-x-y}$ in a roughly triangular region with limits of x=0, y=0; x=0, y≈2/3 and x≈2/3, y=0. Magnetic behavior consistent with tri-valent cerium moments is observed at these limits with ferromagnetic ordering present for x=0, y=2/3. Cubic $Ce_8Pd_{24}Sn$ has an effective high temperature moment of 2.49(4)μB and anti-ferromagnetic ordering at 7.5K. A hexagonal phase dominates the composition "$Ce_4Pd_7Sn_4$", but a structural solution has remained elusive. An effective cerium moment of 2.53(4)μB is observed in "$Ce_4Pd_7Sn_4$" with a Weiss constant of -23K, suggesting antiferromagnetic interactions, but no ordering is observed above 4.2K.

| 14. SUBJECT TERMS | 15. NUMBER OF PAGES |
|---|---|
| cerium intermetallic, magnetic susceptibility | 30 |
| | 16. PRICE CODE |

| 17. SECURITY CLASSIFICATION OF REPORT | 18. SECURITY CLASSIFICATION OF THIS PAGE | 19. SECURITY CLASSIFICATION OF ABSTRACT | 20. LIMITATION OF ABSTRACT |
|---|---|---|---|
| Unclassified | Unclassified | Unclassified | |

**OFFICE OF NAVAL RESEARCH**

Grant or Contract N00014-93-1-0904

R&T Code 3134037ess08
Scientific Officer: Dr. John Pazik

Technical Report No. 25

# "Magnetic Behavior of New Ce-Pd-Sn Ternary Compounds"

by

R.A. Gordon and F.J. DiSalvo

Submitted to

J. Alloys and Compounds

Cornell University
Department of Chemistry
Ithaca, NY 14853

January 12, 1996

Draft submitted 11/9/95

# Magnetic Behavior of New Ce-Pd-Sn Ternary Compounds

R.A. Gordon and F.J. DiSalvo[1]
*Department of Chemistry,*
*Cornell University, Ithaca, NY 14853-1301*

*Dedicated to Wolfgang Jeitschko on the occasion of his 60th birthday, May 27, 1996.*

Submitted.....Journal of Alloys and Compounds

---

**Abstract**

We have prepared and measured the magnetic susceptibility of several new ternary compounds in the Ce-Pd-Sn system: $CePd_{0.5}Sn_2$, $Ce_8Pd_{24}Sn$, "$Ce_4Pd_7Sn_4$" and the solid solution based on $Ce_2Pd_2Sn$. In $CePd_{0.5}Sn_2$, an effective magnetic moment of $2.60(3)\mu_B$ is observed but no ordering is apparent above 4.2K. Complete nickel substitution for Pd in $Ce(Pd_{1-x}Ni_x)_{0.5}Sn_2$ results in the known lower limit to the $CeNi_{1-x}Sn_2$ solid solution. We have determined the extent of the solid solution based on $Ce_2Pd_2Sn$ to have the form $Ce_4Pd_{4+2x}Sn_{2-x-y}$ in a roughly triangular region with limits of $x=0$, $y=0$; $x=0$, $y\approx 2/3$ and $x\approx 2/3$, $y=0$. Magnetic behavior consistent with tri-valent cerium moments is observed at these limits with ferromagnetic ordering present for $x = 0$, $y = 2/3$. Cubic $Ce_8Pd_{24}Sn$ has an effective high temperature moment of $2.49(4)\mu_B$ and anti-ferromagnetic ordering at 7.5K. A hexagonal phase dominates the composition "$Ce_4Pd_7Sn_4$", but a structural solution has remained elusive. An effective cerium moment of $2.53(4)\mu_B$ is observed in "$Ce_4Pd_7Sn_4$" with a Weiss constant of -23K, suggesting anti-ferromagnetic interactions, but no ordering is observed above 4.2K.

---

Keywords: cerium intermetallic, magnetic susceptibility

---

[1] corresponding author

## 1. Introduction

In the Ce-Ni-Sn ternary system [1], there are 2 intermediate valent (IV) binaries, CeNi [2] and (albeit borderline IV) $CeSn_3$ [3]. If one considers a line of composition which joins these two binaries, one notes that several ternary phases which exhibit related Kondo behavior lie near this line. Dense Kondo behavior is observed in $Ce_2Ni_2Sn$ [4,5] while CeNiSn [6,7] is a Kondo insulator and intermediate valent behavior is reported for $Ce_3Ni_2Sn_7$ [1]. Complete palladium substitution for Ni has been reported in CeNi [2], $Ce_2Ni_2Sn$ [5] and CeNiSn [6] with anti-ferromagnetism reported in CePdSn [6] and ferromagnetism in CePd [2] and $Ce_2Pd_2Sn$ [5].

In the Ce-Pd-Sn ternary system, three ternaries are known: CePdSn [6], $CePd_2Sn_2$ [8] and $Ce_2Pd_2Sn$ [5]. The binaries which exhibit intermediate valent behavior are $CePd_3$ [9] and, again, $CeSn_3$. As part of our ongoing search for new materials which exhibit unusual electronic behavior like intermediate valence [5, 10, 11], we have examined the region of the Ce-Pd-Sn ternary phase diagram that lies near the composition line of 25 at% Ce. In principle, this line could be considered a demarcation between tri-valent and tetra-valent cerium behavior (i.e. hypothetical compositions at which the Fermi level for the material would lie at the energy of the $4f^1$ state). In practice, the boundary is expected to encompass a region (Fig. 1) since the line considers only electron counting and neglects structural effects [12, 13]. Discussed below are the results of our search in such a region of the Ce-Pd-Sn phase diagram near 25 at% cerium.

## 2. Experimental

Samples were prepared by arc-melting elements of at least 99.9% purity on a tantalum-coated, water-cooled copper hearth under flowing, Ti-gettered argon as previously described [5]. Samples were then placed in sections of tantalum tubing and sealed in quartz under vacuum for anneal. Annealing temperatures and durations varied from 5 weeks at 750°C to 4 weeks at 900°C with the more Pd-rich samples typically receiving the higher temperature.

Samples were examined by powder diffraction methods using a SCINTAG $\theta/2\theta$ diffractometer, Cu $K\alpha 1$ radiation and silicon as an internal standard. Indexing of the diffraction patterns was done using the program TREOR90 [14] and the lattice constants obtained thereby were least-squares refined. Magnetic susceptibility measurements were performed using a Faraday balance and fit to a Curie-Weiss expression, $\chi = \chi_o + C/(T - \theta)$ as described elsewhere [5]. Resistivity measurements on $Ce_8Pd_{24}Sn$ were done by a four-probe technique on a rectangular section 6.0mm x 3.5mm x 1.2mm in size by soldering on indium contacts ultrasonically. Density measurements were performed by a gas displacement technique [15].

## 3. Results and Discussion

With the exception of $Ce_8Pd_{24}Sn$, the Ce-Pd-Sn ternary compounds prepared are brittle, exhibiting a tendency to crack severely on cooling, and are also mildly air-sensitive. Exposed surfaces are initially silvery metallic in appearance but turn a dark gray after several days exposure to air. Beads prepared in the $Ce_4Pd_{4+2x}Sn_{2-x-y}$ alloy range exhibit striations on their surfaces, suggesting regions of parallel grain growth. Beads of composition $CePd_{0.5}Sn_2$ and "$Ce_4Pd_7Sn_4$" grow numerous needle-shaped crystals up to a few millimeters in length across

their surfaces on solidification in the arc furnace. When cracked apart, these samples appear to have columnar grain growth radiating out from the base of the bead. All samples could be ground easily either in an argon-filled glove box or under acetone for X-ray work. A summary of cell and magnetic data for these compounds is given in Table 1.

*$Ce(Pd_{1-x}Ni_x)_{0.5}Sn_2$*

The powder diffraction pattern for material from a bead of composition $CePd_{0.5}Sn_2$ annealed 5 weeks at 750°C and ground in an argon-filled glove box could be completely indexed to an orthorhombic cell 4.5636(5) x 17.584(2) x 4.5059(5) $Å^3$ consistent with the cells reported for the endpoints of the $LaPd_xSn_2$ solid solution ($0.34 < x < 0.68$) [16]. We did not examine $CePd_{0.5}Sn_2$ for the existence of a comparable alloy range. Nickel substitution for Pd was examined in the cerium compound and, based on powder diffraction data, appears to substitute completely to form the reported lower limit to the $CeNi_xSn_2$ solid solution ($0.5 < x < 1$) [1]. No structural or magnetic data, however, was reported for $CeNi_xSn_2$ for $x < 1$. Table 2 lists the cell parameters for the compositions prepared. These $Ce(Pd_{1-x}Ni_x)_{0.5}Sn_2$ materials are assumed to adopt the $CeNiSi_2$ structure type as reported for the lanthanum-based alloy range and $CeNiSn_2$. From the linear dependence of cell volume on concentration of nickel (Fig. 2), we do not anticipate any change in valence of the cerium on substitution of Ni for Pd which would manifest as a deviation from linearity (Vegard behavior) [5].

Magnetic susceptibility data on $CePd_{0.5}Sn_2$ were collected on loose, powdered material obtained from a bead annealed 5 weeks at 750°C. The inverse of the magnetic susceptibility is shown in Figure 3. The cooling data exhibits several discontinuities involving an increase in $\chi$

which result from re-orientation of the loose powder in the applied magnetic field [5]. If the cerium magnetic moment is anisotropic, through spin-orbit coupling and interaction with the crystal electric field, and the anisotropy is large, then small single-crystalline particles will experience a torque forcing them to re-align in the applied field if the particles are free to move. Since the heating data does not exhibit any such discontinuities, the oriented particles remain fixed in the positions attained on cooling to 4.2K. Complete orientation along a crystallographic direction is not assured owing to the polycrystalline nature of the starting material. Fitting the heating data above 100K to a Curie-Weiss expression yields an effective high temperature moment of $2.60(3)\mu_B$ per cerium and $\theta$ = 8(2)K, suggesting some weak, ferromagnetic exchange. The effective moment, while larger than that expected for a free $Ce^{+3}$ ion ($4f^1$) ($2.54\mu_B$) is still reasonable for a $4f^1$ configuration in solids. The inverse magnetic susceptibility for $CeNi_{0.5}Sn_2$ is displayed in Figure 4. Data were collected on a single piece of $CeNi_{0.5}Sn_2$ rather than powder. As anticipated from the dependence of cell volume on nickel concentration, the cerium moment is comparable to that for $CePd_{0.5}Sn_2$ with a fit to data above 100K yielding an effective moment of $2.60(2)\mu_B$ and a $\theta$ of -1(2)K. The moment obtained is somewhat larger than that reported for $CeNiSn_2$ ($\mu$ = $2.43\mu_B$, $\theta$ = 5K). Neither the Pd nor the Ni sample exhibits any apparent magnetic ordering above 4.2K. Below 100K, however, there is some deviation from Curie-Weiss behavior (decreasing slope in $\chi^{-1}$) that can be ascribed to thermal depopulation of cerium f-states split by interaction with the crystal electric field.

*$Ce_8Pd_{24}Sn$*

This compound was prepared as part of a series $Ce_8Pd_{24}M$ with M = (Ga, In, Sn, Pb, Sb and Bi) [17]. We include some discussion of it here for completeness. The cubic structure of $Ce_8Pd_{24}Sn$ (Fig. 5) is obtained from the $Cu_3Au$ structure of $CePd_3$ by incorporating one Sn atom at the body-centre site of one out of eight $CePd_3$ cells. Doing so results in the Pd atoms being pushed outward from the face of the cube defined by the cerium atoms, producing a cubic super-cell with a lattice constant slightly more than twice that of $CePd_3$.

The inverse of the magnetic susceptibility from 4.2K to 320K of $Ce_8Pd_{24}Sn$ is given in Figure 6 with an inset showing the susceptibility from 4.2K to 30K. Anti-ferromagnetic ordering occurs at 7.5K. Fitting the magnetic susceptibility above 100K yields an effective cerium moment of $2.49(4)\mu_B$ and anti-ferromagnetic exchange ($\theta$ = -11(3)K). Deviations from Curie behavior below 100K can be attributed to thermal depopulation of crystal field split cerium 4f states resulting in a temperature dependent moment. Decreasing scattering of conduction electrons also results from thermal depopulation of the crystal field split 4f states, producing the gradually increasing slope on cooling in the resistivity of $Ce_8Pd_{24}Sn$ (Fig. 7) between 100K and 30K. An abrupt change in the slope of the resistivity occurs at 7.5K, consistent with the onset of anti-ferromagnetic ordering. There is no apparent evidence of any Kondo interaction in $Ce_8Pd_{24}Sn$ even though it is close in composition to the well-known intermediate valent compound, $CePd_3$.

*$Ce_4Pd_{4+2x}Sn_{2-x-y}$*

It is possible to substitute Pd for Sn in $U_2Pd_2Sn$ as $U_2Pd_{2+x}Sn_{1-x}$ [18]; however, in our study on the alloy range based on $Ce_2Pd_2Sn$, we observed a more extensive solid solution (Table 1) of the compositional form $Ce_4Pd_{4+2x}Sn_{2-x-y}$. A simple substitution of one Pd for one Sn can be easily understood but something more complicated must be occurring to explain the more extensive observed alloy range.

The region the solid solution comprises is roughly triangular with end point vertices at (x,y) = (0, 2/3) and (2/3, 0) and the parent compound $Ce_2Pd_2Sn$. To obtain a single phase powder pattern, a sample of composition $Ce_4Pd_4Sn_{4/3}$ (0, 2/3) was annealed at 900°C for 4 weeks while the sample at composition $Ce_4Pd_{16/3}Sn_{4/3}$ (2/3, 0) could be obtained single phase by powder diffraction after 4 weeks anneal at 750°C. The results of density measurements on the end points are: (0, 2/3), $\rho$ = 8.6(1)g/cm$^3$; (2/3, 0), $\rho$ = 9.0(1)g/cm$^3$. If one interprets the compositions $Ce_4Pd_{4+2x}Sn_{2-x-y}$ as the unit cell contents (i.e. Z = 2 in the cell of $Ce_2Pd_2Sn$), then one can calculate densities (formula weight divided by unit cell volume from Table 1) for the (0, 2/3) and (2/3, 0) compositions. These values are 7.94g/cm$^3$ and 8.95g/cm$^3$ for the (0, 2/3) and (2/3, 0) samples respectively. The density of the (2/3, 0) sample is consistent with the calculated value, but that of the (0, 2/3) sample is not.

If the Sn-deficient sites in the (0, 2/3) sample were vacant, one would expect a contraction of the unit cell compared to the parent $Ce_2Pd_2Sn$. Instead, a small expansion is observed (Table 1). If the Sn-deficient sites were not vacant but, instead, occupied as one would expect for a direct atom for atom substitution and occupied in such a fashion as to preserve the overall composition (i.e. $Ce_4Pd_4(Sn_{4/3}[Ce_{3/7}Pd_{3/7}Sn_{1/7}]_{2/3})$ rather than $Ce_4Pd_4(Sn_{4/3}[\ ]_{2/3})$ ) then

the density would be 8.51g/cm$^3$, consistent with the observed density. One can calculate an effective covalent radius for [ ] = ($Ce_{3/7}Pd_{3/7}$ $Sn_{1/7}$) by averaging the covalent radii for the constituent elements (Ce, 1.65Å; Pd, 1.28Å; Sn, 1.41Å) [19]. This average radius is 1.46Å, and is 0.05Å larger than the covalent radius of Sn. This correlates with the small expansion of the unit cell relative to stoichiometric $Ce_2Pd_2Sn$.

The measured density of the (2/3, 0) sample is consistent with that calculated based on the composition and size of the unit cell. The nature of the substitution, however, can not be a simple exchange of one Pd for one Sn since this composition contains more palladium. We propose that a pair of palladium atoms occupies the space formerly occupied by a tin atom. Our model for such double occupancy follows. Inter-palladium distances in intermetallic compounds comparable to the Pd-Pd distance in palladium metal, 2.751Å, [20] have been observed in a number of Pd-rich Ce-Pd-Sb ternary compounds: $Ce_3Pd_6Sb_5$ ($d_{Pd\text{-}Pd}$ = 2.762Å) [10], $Ce_2Pd_9Sb_3$ (2.710Å) [21] and $Ce_8Pd_{24}Sb$ (2.765Å) [11] and have also been observed in the $GdPd_3As_2$ structure type (2.754Å) [22]. Based on the cell parameters of the (2/3, 0) sample and the atomic positions of $U_2Rh_2Sn$ [23], we estimate the size of the tetragonal prism formed by the cerium atoms around the tin site in the (2/3, 0) sample to be 4.014Å x 4.014Å x 4.0597Å. In Figure 8, we compare three of these prisms adjoining along ***c*** (Fig. 8b) with three similar prisms (Fig. 8a) from $Ce_2Pd_2Sn$ (again calculated based on $U_2Rh_2Sn$) and with a corresponding section (Fig. 8c) along ***c*** of $Ce_8Pd_{24}Sn$. In crystallographic terms, we model this endpoint of the alloy range by allowing a 2/3 random occupancy of the Sn site (Wyckoff position 2a, x = 0, y = 0, z = 0) and a 1/3 occupancy of the Wyckoff site 4e (0, 0, 0.338) in the space group P4/mbm (No. 127). This places two palladium atoms 2.744Å apart parallel to the *c*-axis, centred at the tin

vacancies. The similarity of this model to the section of $Ce_8Pd_{24}Sn$ (Fig. 8c) is quite apparent. In examining the distances from these substituted palladium atoms to the near neighbours, we find $d_{Pd\text{-}Sn}$ = 2.688Å and $d_{Pd\text{-}Ce}$ = 2.914Å. Both of these distances are comparable to the sums of the respective covalent radii, 2.69Å and 2.93Å [19]. This model for the Pd-rich region of the $Ce_4Pd_{4+2x}Sn_{2-x-y}$ solid solution is consistent with the observed density data. An alternative model in which a single palladium atom substitutes for tin on the 2a site, and the second palladium atom occupies an interstitial position away from the 2a site, is harder to justify. The $Ce_2Pd_2Sn$ structure (Figure 9) offers no interstitial positions of appreciable volume (other than near the 2a site), hence such a defect is unlikely.

The magnetic behavior of the endpoints to the $Ce_4Pd_{4+2x}Sn_{2-x-y}$ solid solution differ. For the (0, 2/3) sample, ferromagnetic ordering occurs (Fig. 10) at $T_c$ = 7K. The effective high temperature moment (T > 80K) of 2.54(1)$\mu_B$ per cerium is equal to the free ion value and a Weiss constant of 14(1)K concurs with the ferromagnetic ordering. The ferromagnetic ordering temperature is larger than in the parent $Ce_2Pd_2Sn$ ($T_c \sim$ 4K [5]) and comparable to the ordering temperature in ferromagnetic CePd (6.6K [2]) which it approaches in composition. The inverse magnetic susceptibility for the (2/3, 0) endpoint (Fig. 11) does not exhibit any magnetic ordering above 4.2K. Shown in the inset to Fig. 10 are discontinuities attributed to a re-orienting of the single piece (not powder) measured, the orientation of which could not be sustained on warming. A preferred direction for grain growth in the arc-melted bead would result in a torque on even a single piece 40mg in mass if the anisotropy of the moments is large. Fitting the susceptibility data collected on cooling for T > 70K yields an effective cerium moment of 2.47(2)$\mu_B$ and a $\theta$ of -6(1)K, while fitting the heating data above 130K yields an effective cerium moment of

2.46(6)$\mu_B$ and $\theta$ = -4(6)K. Both are consistent with each other and the free $Ce^{+3}$ ion value of 2.54$\mu_B$ for a $4f^1$ electronic configuration.

*"$Ce_4Pd_7Sn_4$"*

Attempts to prepare a stannide analogue to $CePd_2In$ [25] invariably resulted in a multi-phase product when the desired 1:2:1 stoichiometry was used. An hexagonal majority phase is present in as-cast samples of 1:2:1 composition and was still present after anneal at temperatures below 1000°C (melting occurred above 1000°C) so nearby compositions were examined in an effort to locate this phase. At the 4:7:4 composition, we were able to obtain the largest fraction of the hexagonal phase (largest unindexed peak intensity 5% of the most intense indexed peak) after 10 days anneal at 900°C. Other nearby compositions examined were: 2:3:2, 5:8:5, 5:9:6, 25:48:27, 3:5:2 and 2:5:3. The powder diffraction peaks selected for initial indexing were common ones to the patterns for these samples. Two hexagonal unit cells were obtained from TREOR90 [14], both with comparable *c* values as in Table 1 but one with $a$ = 9.322Å and the other with $a$ = 8.073Å. The latter $a$ parameter is $(\sqrt{3})/2$ of the former so that the two cells are related by a 30° rotation. A single crystal of dimensions 0.212 x 0.057 x 0.057 $mm^3$ was obtained after melting the 25:48:27 sample in a tantalum tube and slow cooling over 24 hours. Precession and single crystal work suggested the 8.073Å x 8.073Å x 16.797Å cell was appropriate but we have been unable to solve the structure from the data set collected.

Magnetic measurements were performed on a single piece (32.8(1)mg) of the 4:7:4 sample (Fig. 12). Susceptibility data above 80K fit to a Curie-Weiss expression yielded an effective high temperature moment of 2.53(4)$\mu_B$ per cerium and suggests some anti-

ferromagnetic interactions from a negative Weiss parameter of -23(3)K. However, the extent of any crystal field contribution to the Weiss parameter is unknown, so $\theta$, again, cannot be strictly interpreted as due to an exchange energy. Deviations from linear behavior below 80K likely result from crystal field effects.

## 4. Conclusions

We have prepared 3 new ternaries in the Ce-Pd-Sn ternary system and examined the solid solution based on the known $Ce_2Pd_2Sn$ compound. The ternary compound (alloy), $CePd_{0.5}Sn_2$ exhibits no ordering in its magnetic susceptibility. Nickel substitution in $Ce(Pd_{1-x}Ni_x)_{0.5}Sn_2$ results in $CeNi_{0.5}Sn_2$, the lower limit of the $CeNi_xSn_2$ solid solution. The solid solution region based on the $Ce_2Pd_2Sn$ compound has the form $Ce_4Pd_{4+2x}Sn_{2-x-y}$ with approximate limits of $x = 0$, $y = 2/3$ and $x = 2/3$, $y = 0$. At the (0, 2/3) limit, ferromagnetic ordering is observed with $T_c = 7K$. No magnetic ordering is observed in the susceptibility of the (2/3, 0) limit. The cubic compound $Ce_8Pd_{24}Sn$ exhibits anti-ferromagnetic ordering at 7.5K and, despite its proximity to $CePd_3$, displays no behavior that can be associated with a Kondo interaction. A hexagonal phase was found near the composition "$Ce_4Pd_7Sn_4$" but the structure is currently unsolved. Effective high temperature magnetic moments consistent with tri-valent cerium is observed in all materials studied here.

## 5. Acknowledgements

We appreciate the support of the Office of Naval Research. We would like to thank N.E. Brese and R. Pöttgen for valued advice and some assistance during our attempts to solve the "4:7:4" crystal structure.

## References


[1] R.V. Skolozdra and L.P. Komarovskaya, *Izv. Akad. Nauk SSSR. Metally, (2)* (1988) 214.

[2] G.L. Nieva, J.G. Sereni, M. Afyouni, G. Schmerber and J.P. Kappler, *Z. Phys. B - Cond. Mat., 70* (1988) 181.

[3] J.M. Lawrence, P.S. Riseborough and R.D. Parks, *Rep. Prog. Phys., 44* (1981) 1.

[4] F. Fourgeot, B. Chevalier, P. Gravereau, L. Fournès and J. Etourneau, *J. Alloys Comp., 218* (1995) 90.

[5] R.A. Gordon, Y. Ijiri, C.M. Spencer and F.J. DiSalvo, *J. Alloys Comp., 224* (1995) 101.

[6] M. Kasaya, T. Tani, F. Iga and T. Kasuya, *J. Magn. Magn. Mater., 76&77* (1988) 278.

[7] T. Takabatake, F. Teshima, H. Fujii, S. Nishigori, T. Suzuki, T. Fujita, Y. Yamaguchi, J. Sakurai and D. Jaccard, *Phys. Rev. B, 41* (1990) 9607.

[8] W.P. Beyerman, M.F. Hundley, P.C. Canfield, C. Godart, M. Selsane, Z. Fisk, J.L. Smith and J.D. Thompson, *Physica B, 171* (1991) 373.

[9] P.A. Veenhuizen, F. Yang, H. van Nassou and F.R. de Boer, *J. Magn. Magn. Mater., 63&64* (1987) 567.

[10] R.A. Gordon, F.J. DiSalvo and R. Pöttgen, *J. Alloys Comp., 228* (1995) 16.

[11] R.A. Gordon and F.J. DiSalvo, *Z. Naturforsch. B,* in press.

[12] R.A. Neifeld, M. Croft, T. Mihalisin, C.U. Segre, M. Madigan, M.S. Torikachvili, M.B. Maple and L.E. DeLong, *Phys. Rev. B, 32* (1985) 6928.

[13] J.G. Sereni and O. Trovarelli, *J. Magn. Magn. Mater., 140-144* (1995) 885.

[14] P.E. Werner, L. Eriksson and M. Westdahl, *J. Appl. Crystallogr., 18* (1985) 367.

[15] M.Y. Chern, R.D. Mariani, D.A. Vennos and F.J. DiSalvo, *Rev. Sci. Instrum., 61* (1990) 1733.

[16] M. François, G. Venturini, B. Malaman and B. Roques, *J. Less-Common Met., 160* (1990) 197.

[17] R.A. Gordon, C.D.W. Jones, G. Alexander and F. J. DiSalvo, *Physica B*, submitted.

[18] F. Mirambet, B. Chevalier, L. Fournès, P. Gravereau and J. Etourneau, *J. Alloys Comp., 203* (1994) 29.

[19] R.T. Sanderson, *Inorganic Chemistry*, Reinhold Publishing Corporation, 1967, 74.

[20] J. Donohue, *The Structures of the Elements*, Wiley, New York, 1974, 216.

[21] R.A. Gordon, F.J. DiSalvo, R. Pöttgen and N.E. Brese, *Faraday Transactions*, submitted.

[22] P. Quebe and W. Jeitschko, *J. Solid State Chem., 115* (1995) 37.

[23] F. Mirambet, P. Gravereau, B. Chevalier, L. Trut and J. Etourneau, *J. Alloys Comp., 191* (1993) L1.

[24] E. Dowty, ATOMS 3.1 for Windows, Shape Software, Kingsport TN, 1994.

[25] B. Xue, F. Hulliger, Ch. Baerlocher and M. Estermann, *J. Alloys Comp., 191* (1993) L9.

**Table 1**
Summary of lattice parameters and magnetic data.

| compound | cell | *a*/Å | *b*/Å | *c*/Å | Vol./Å$^3$ | $\mu_{eff}/\mu_B$ | $\theta$/K |
|---|---|---|---|---|---|---|---|
| $CePd_{0.5}Sn_2$ | ortho. | 4.5636(5) | 17.584(2) | 4.5059(5) | 361.87(7) | 2.60(3) | 8(2) |
| $Ce_4Pd_{4+2x}Sn_{2-x-y}$ | | | | | | | |
| x=0,y=0[†] | tetrag. | 7.774(1) | | 3.926(1) | 237.27(7) | 2.62(2) | 18(1) |
| x=0,y=2/3 | " | 7.7968(7) | | 3.9347(4) | 239.19(4) | 2.54(1) | 14(1) |
| x,y=1/3 | " | 7.692(1) | | 4.0165(5) | 237.64(5) | --- | --- |
| x=1/3,y=0 | " | 7.6964(8) | | 4.0235(4) | 238.33(4) | --- | --- |
| x=2/3,y=0 | " | 7.6683(6) | | 4.0597(3) | 238.72(3) | 2.47(2) | 6(1) |
| "$Ce_4Pd_7Sn_4$" | hex. | 8.073(1) | | 16.797(3) | 948.1(2) | 2.53(4) | -23(5) |
| $Ce_8Pd_{24}Sn$ | cubic | 8.4446(8) | | | 602.2(1) | 2.49(4) | -11(3) |

[†] from reference [5]

**Table 2**
Cell data for Ni substitution in $Ce(Pd_{1-x}Ni_x)_{0.5}Sn_2$.

| x | *a*/Å | *b*/Å | *c*/Å | Vol./Å$^3$ |
|---|---|---|---|---|
| 0.00 | 4.5636(5) | 17.584(2) | 4.5059(5) | 361.58 |
| 0.25 | 4.5487(5) | 17.495(2) | 4.5070(5) | 358.66 |
| 0.50 | 4.5417(7) | 17.416(3) | 4.4954(7) | 355.57 |
| 0.75 | 4.5335(5) | 17.337(2) | 4.4863(5) | 352.60 |
| 1.00 | 4.5248(5) | 17.251(2) | 4.4753(5) | 349.32 |

**Figure Captions**

Figure 1. The region of the Ce-Pd-Sn phase diagram under investigation.

Figure 2. Variation of cell volume with nickel content for $Ce(Pd_{1-x}Ni_x)_{0.5}Sn_2$.

Figure 3. Inverse magnetic susceptibility of $CePd_{0.5}Sn_2$ from 4.2K to 320K.

Figure 4. Inverse magnetic susceptibility of $CeNi_{0.5}Sn_2$ from 4.2K to 310K.

Figure 5. Perspective view along ***a*** of the unit cell $Ce_8Pd_{24}Sn$ with near-neighbours from adjoining cells. Black Sn atoms mark the corners of the unit cell. Palladium bonds are drawn to emphasise distortions in the structure. Atom designations are: large white spheres, Ce; small gray spheres, Pd; and medium black spheres, Sn.

Figure 6. Inverse susceptibility of $Ce_8Pd_{24}Sn$ from 4.2K to 320K. Inset shows the susceptibility from 4.2K to 30K.

Figure 7. Resistivity of $Ce_8Pd_{24}Sn$ from 4.2K to 293K.

Figure 8. Tin co-ordination enviroments [24] in: (a) $Ce_2Pd_2Sn$, (b) $Ce_4Pd_{16/3}Sn_{4/3}$ (proposed) and (c) $Ce_8Pd_{24}Sn$. Atomic positions in (a) and (b) are based on those for $U_2Rh_2Sn$ and in (c) on $Ce_8Pd_{24}Sb$.

Figure 9. Perspective view down ***c*** of the structure of $Ce_2Pd_2Sn$. Atomic positions are those for $U_2Rh_2Sn$. Atom designations are as in Fig. 5. The outer tin atoms mark the corners of a unit cell.

Figure 10. Inverse magnetic susceptibility for the (0, 2/3) composition of the $Ce_4Pd_{4+2x}Sn_{2-x-y}$ solid solution from 4.2K to 310K.

Figure 11. Inverse magnetic susceptibility for the (2/3, 0) composition of the $Ce_4Pd_{4+2x}Sn_{2-x-y}$ solid solution from 4.2K to 320K.

Figure 12. Inverse magnetic susceptibility of "$Ce_4Pd_7Sn_4$" from 4.2K to 310K.

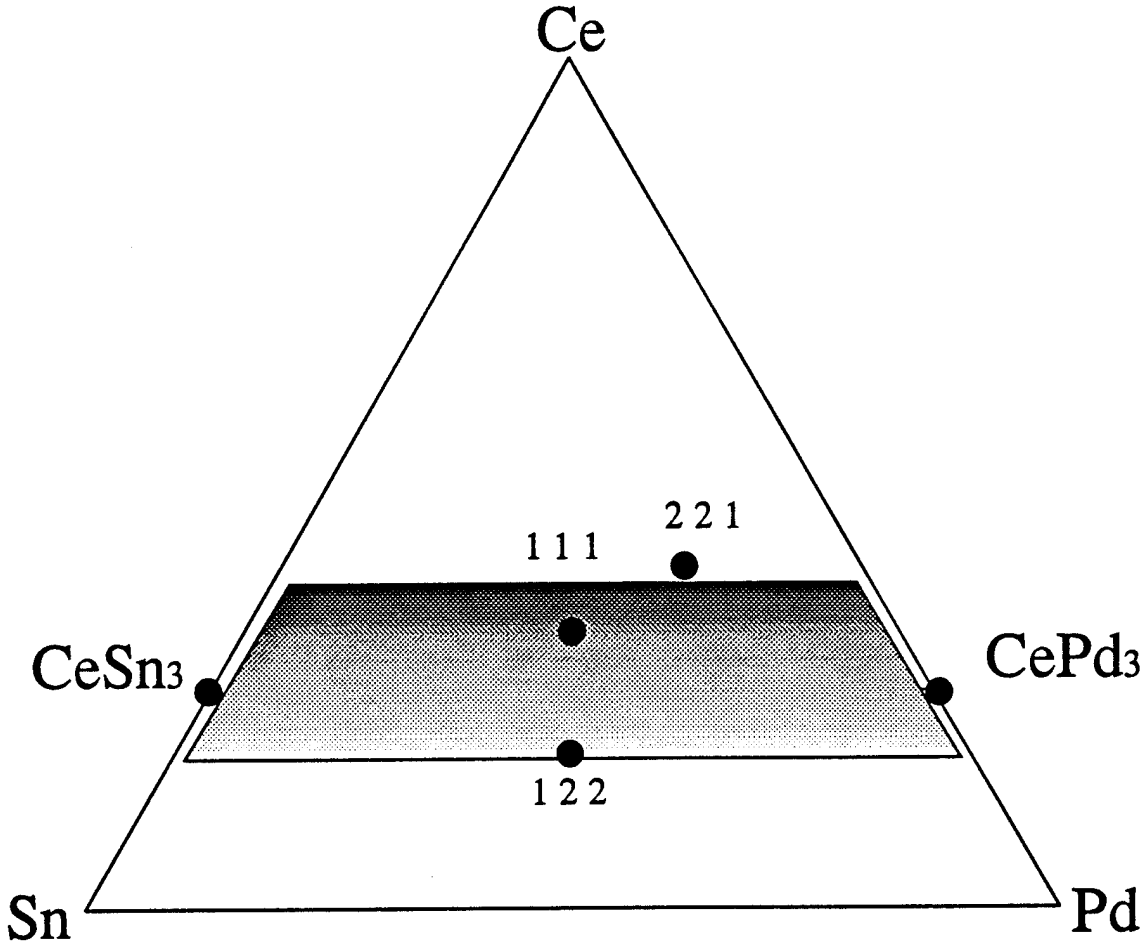
Ce
2 2 1
1 1 1
CeSn3
CePd3
1 2 2
Sn
Pd

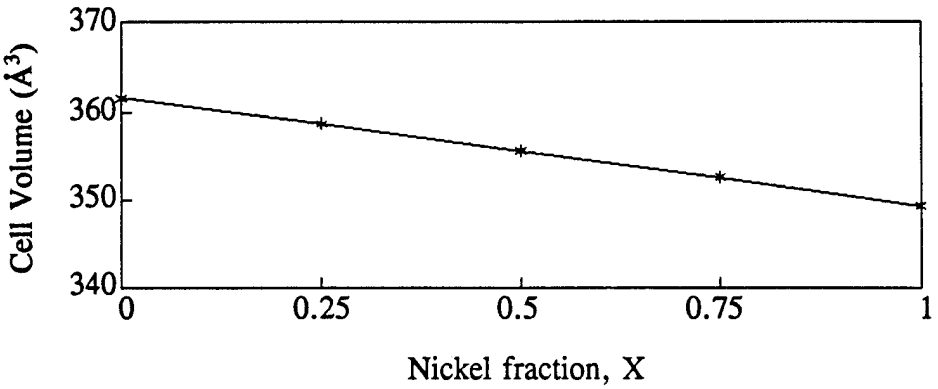
370
360
350
340
Cell Volume (Å³)
0
0.25
0.5
0.75
1
Nickel fraction, X

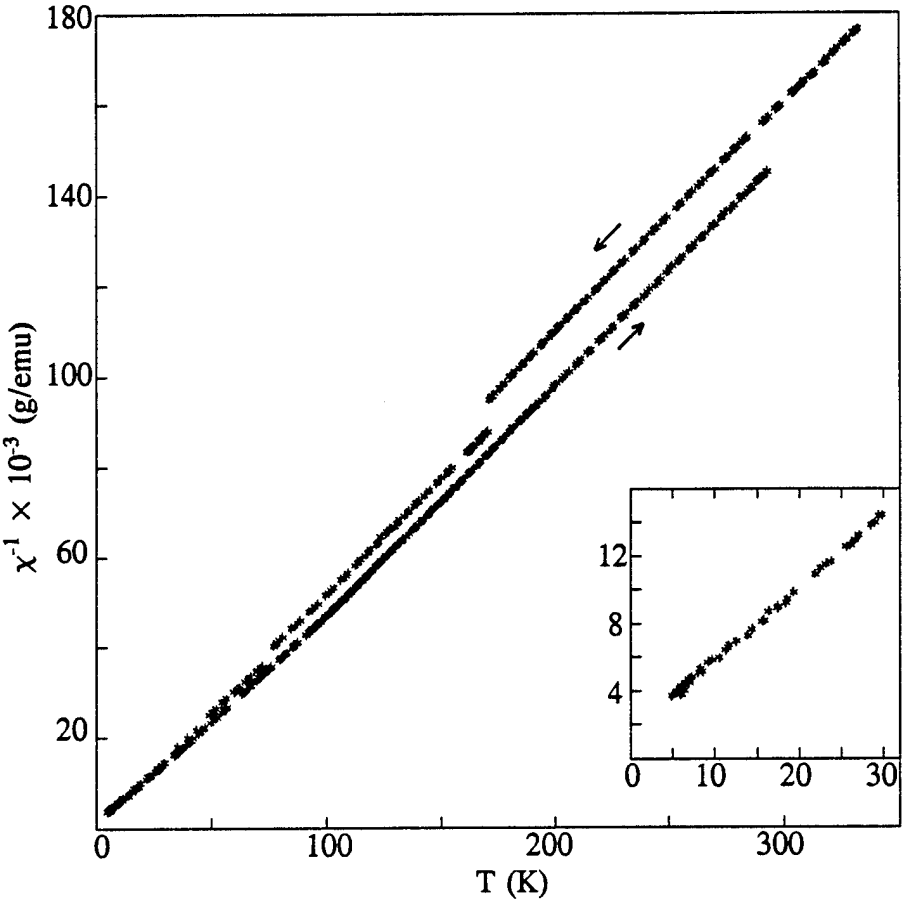
180
140
100
60
20
$\chi^{-1} \times 10^{-3}$ (g/emu)
0
100
200
300
T (K)
12
8
4
0
10
20
30

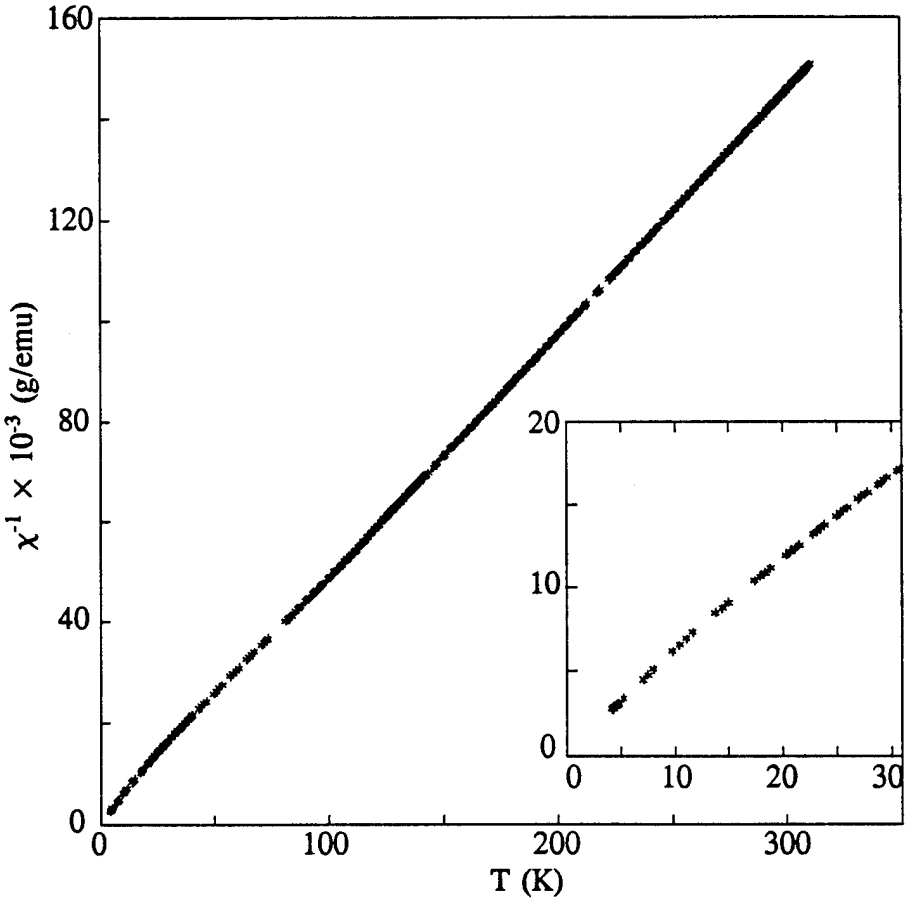
160
120
80
40
0
$\chi^{-1} \times 10^{-3}$ (g/emu)
0
100
200
300
T (K)
20
10
0
0
10
20
30

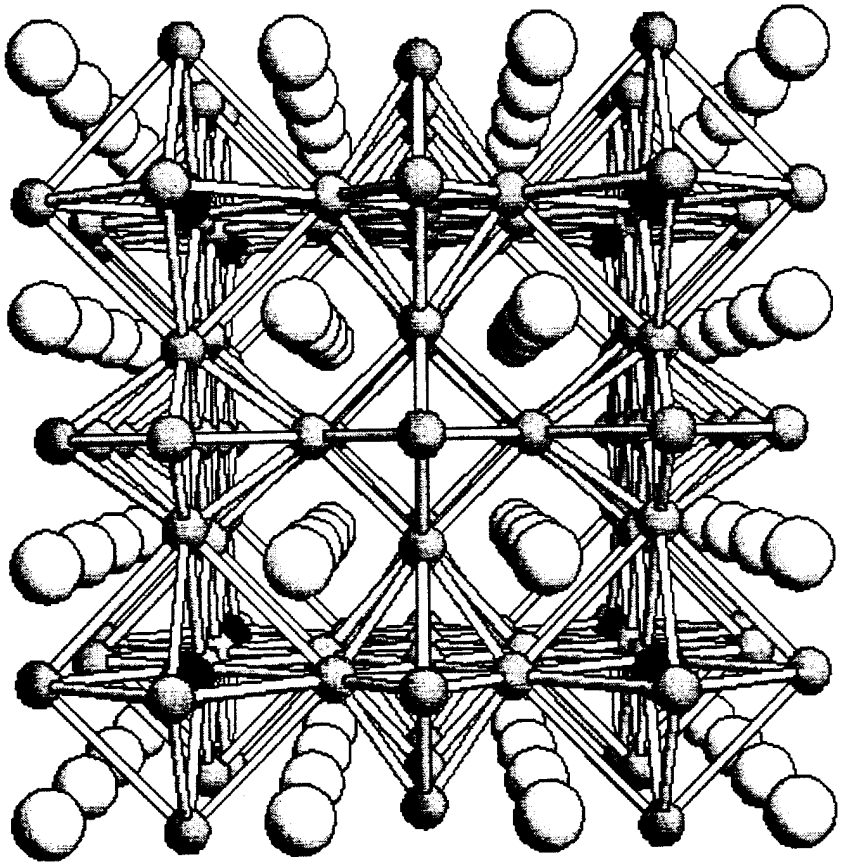

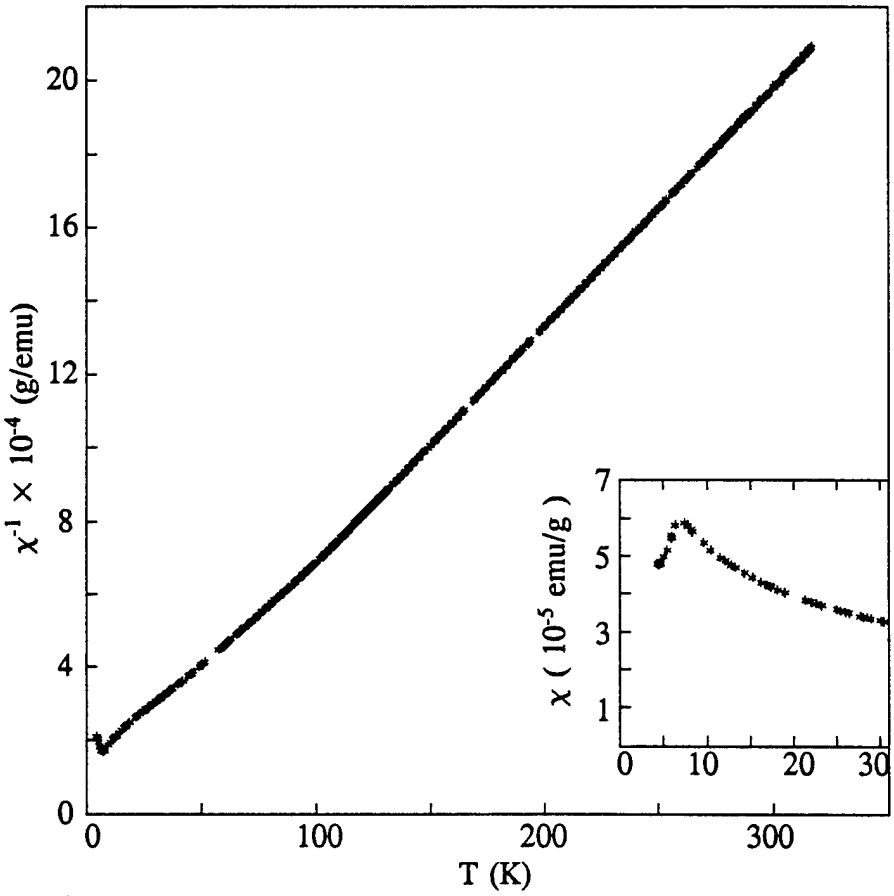
20
16
12
8
4
0
$\chi^{-1} \times 10^{-4}$ (g/emu)
0
100
200
300
T (K)
7
5
3
1
$\chi$ ( $10^{-5}$ emu/g )
0
10
20
30

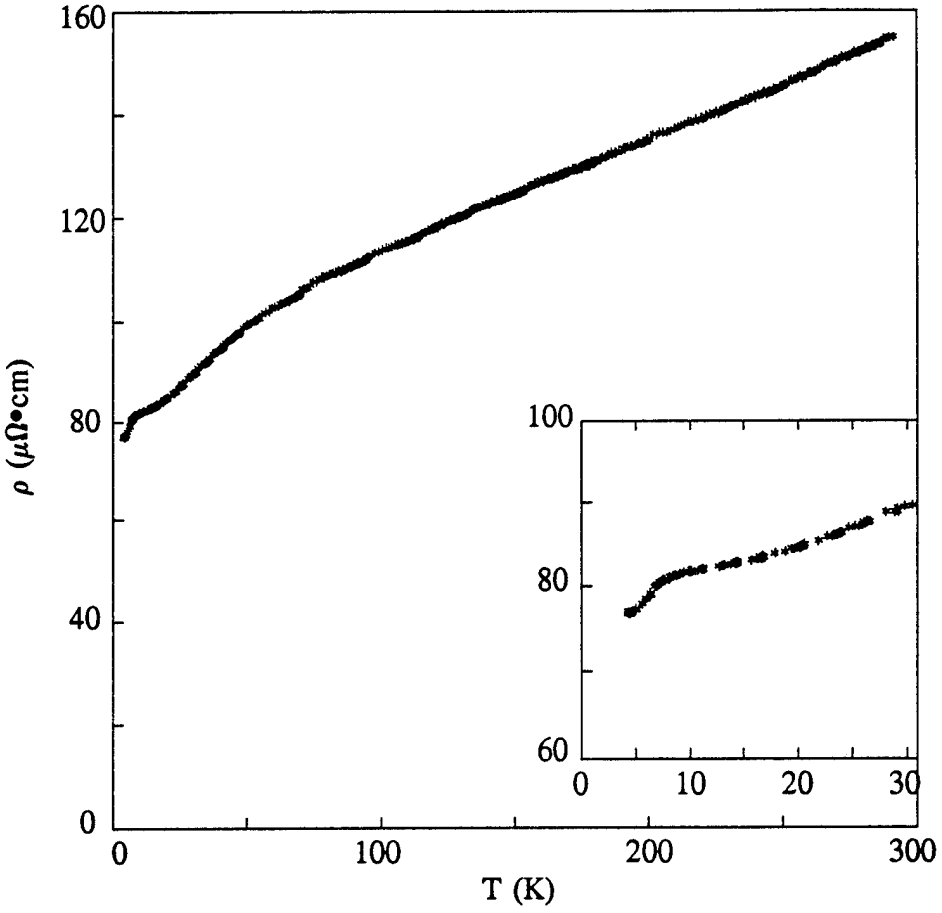
160
120
80
40
0
ρ (μΩ•cm)
0
100
200
300
T (K)
100
80
60
0
10
20
30

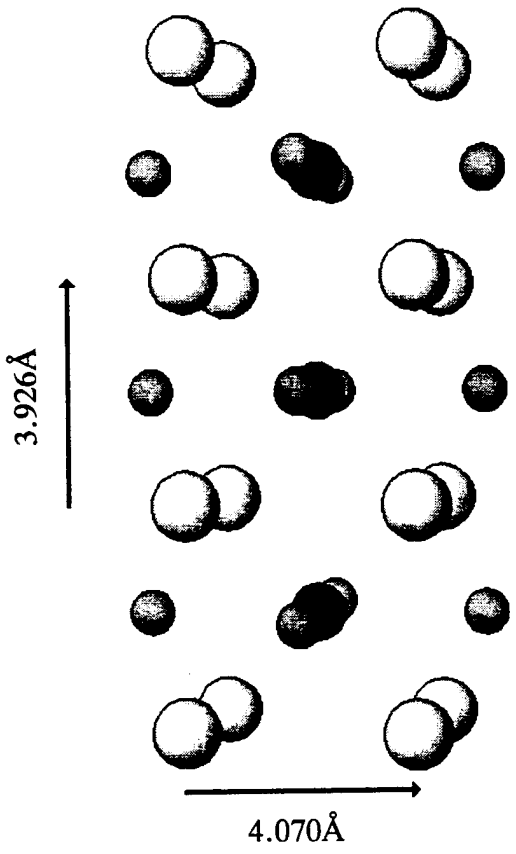
3.926Å
4.070Å

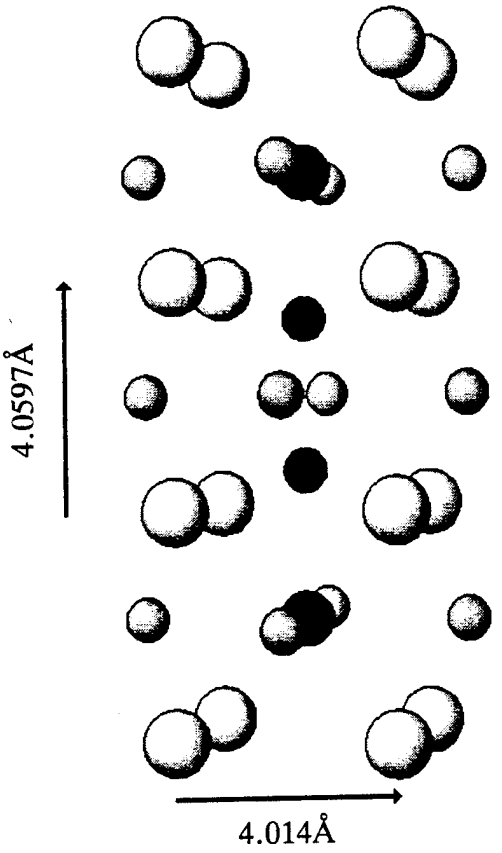
4.0597Å
4.014Å

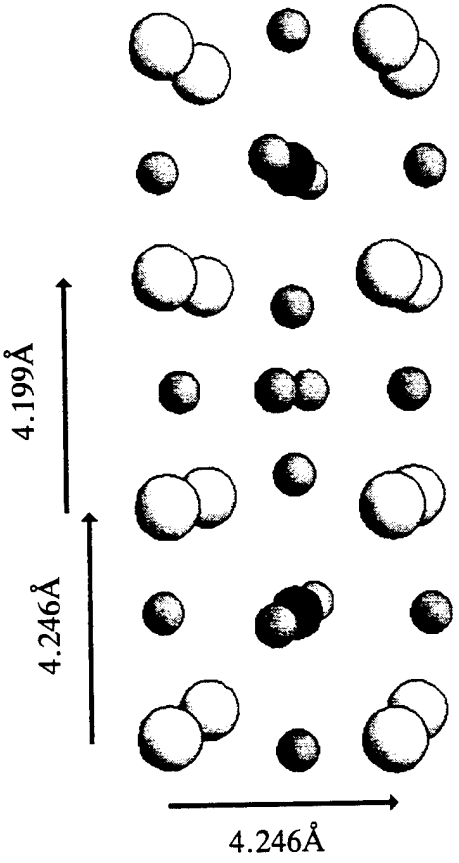
4.199Å
4.246Å
4.246Å

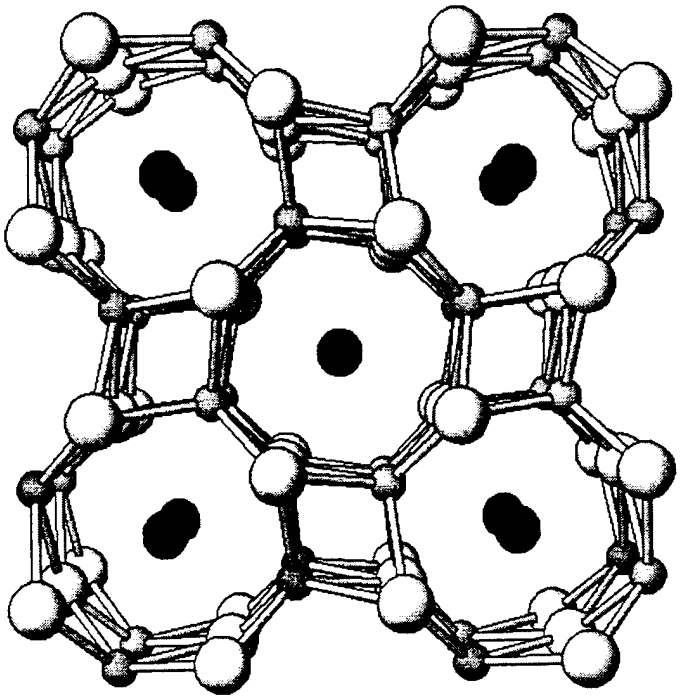

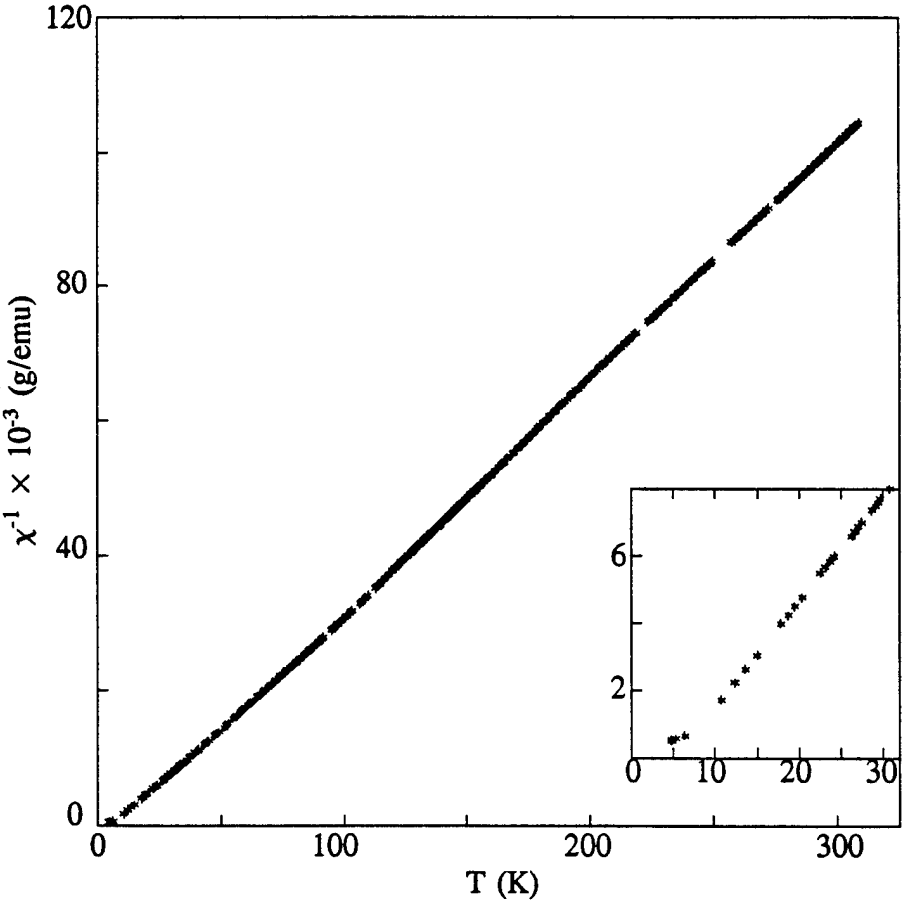
120
80
40
0
$\chi^{-1} \times 10^{-3}$ (g/emu)
0
100
200
300
T (K)
6
2
0
10
20
30

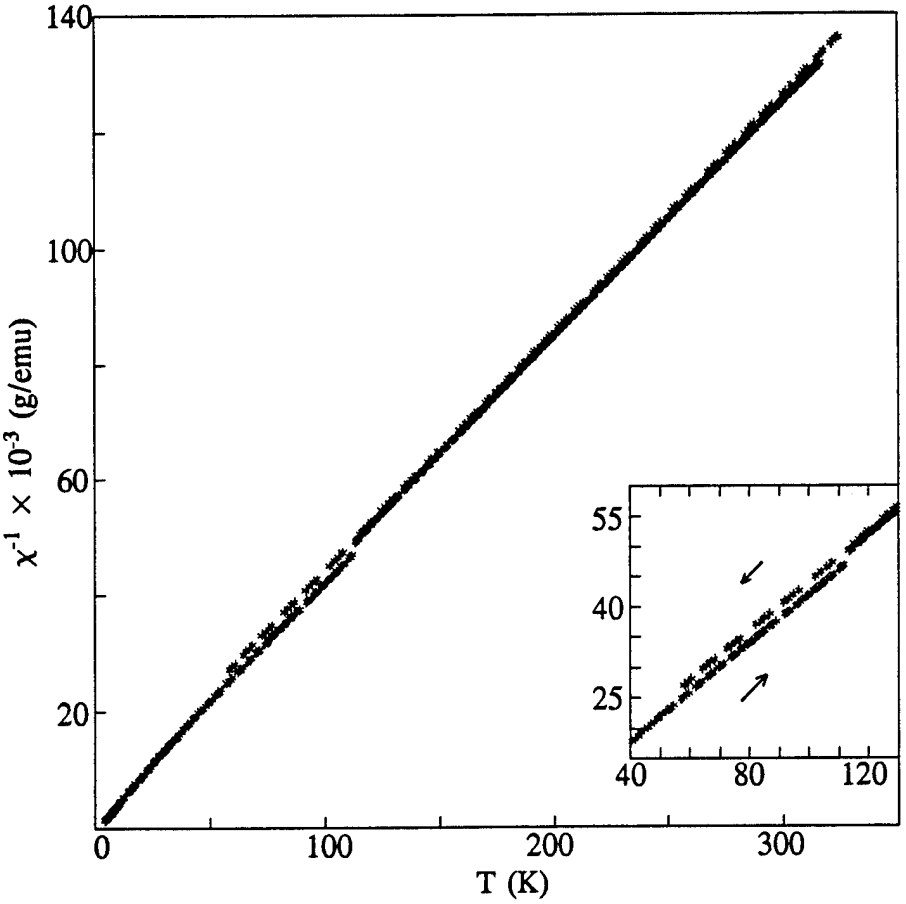
140
100
60
20
$\chi^{-1} \times 10^{-3}$ (g/emu)
0
100
200
300
T (K)
55
40
25
40
80
120

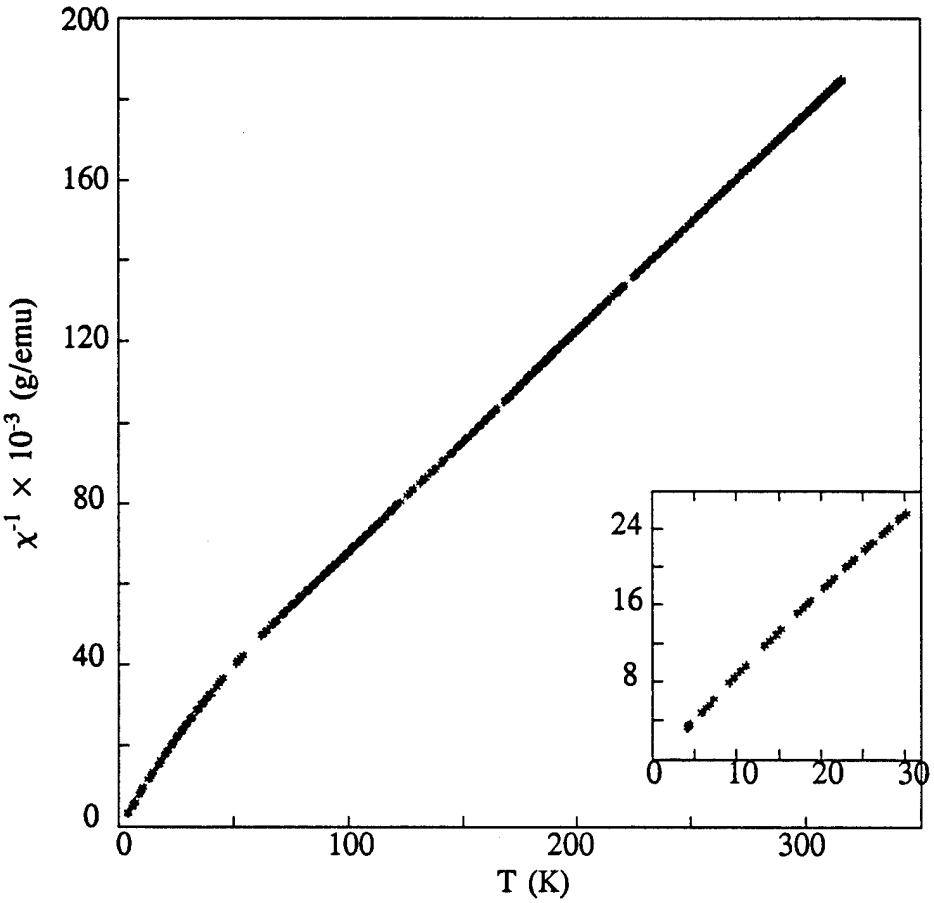
200
160
120
80
40
0
$\chi^{-1} \times 10^{-3}$ (g/emu)
0
100
200
300
T (K)
24
16
8
0
10
20
30

Technical Report Distribution List

Dr. John C. Pazik (1)*
Physical S&T Division - ONR 331
Office of Naval Research
800 N. Quincy St.
Arlington, VA 22217-5660

Defense Technical Information Ctr (2)
Building 5, Cameron Station
Alexandria, VA 22314

Chemistry Division, Code 385
NAWCWD - China Lake
China Lake, CA 93555-6001

Dr. James S. Murday (1)
Chemistry Division, NRL 6100
Naval Research Laboratory
Washington, DC 20375-5660

Dr. John Fischer (1)

Dr. Peter Seligman (1)
NCCOSC - NRAD
San Diego, CA 92152-5000

Dr. Bernard E. Douda (1)
Crane Division
NAWC
Crane, Indiana 47522-5000

* Number of copies required